



The first step towards intelligent wire arc additive manufacturing: An automatic bead modelling system using machine learning through industrial information integration

Donghong Ding ^{a, #}, Fengyang He ^{b, #}, Lei Yuan ^{b,*}, Zengxi Pan ^b, Lei Wang ^b, Montserrat Ros ^b

^a School of Mechatronics Engineering, Foshan University, Foshan, Guangdong 52800, China

^b Faculty of Engineering & Information Sciences, University of Wollongong, Northfields Avenue, Wollongong, NSW 2522, Australia

ARTICLE INFO

Keywords:

Wire arc additive manufacturing (WAAM)
Bead modelling
Machine learning
Support vector machine (SVM)
Robotic welding

ABSTRACT

Wire Arc Additive Manufacturing (WAAM) has revolutionized the manufacturing paradigm for fabricating medium to large scale metallic parts featuring high buy-to-fly ratios such as aerospace components. As a promising technology for the manufacturing industry, it is necessary to develop an automated WAAM system with high efficiency and low labour cost. Generally, to achieve a fully intelligent WAAM system, the first step is to develop an intelligent weld bead modelling system which is able to provide users with appropriate welding parameters in terms of producing components with high accuracy. Knowledge from many disciplines, such as computer science, material engineering, mechanical engineering, and industrial system engineering, is advantageous to develop such an automated system. Thus, an intelligent bead modelling system was developed by integrating a number of industrial sectors in this study. The bead modelling system includes three critical modules, including data generation module, model creation module, and welding parameter generation module. It is worth mentioning that a novel algorithm using Support Vector Machines (SVM) was proposed for creating the model with a high level of accuracy. Optimal combinations of wire feed rate and travel speed under various temperatures were generated accordingly. The experiment results demonstrated that the system can significantly improve product quality and reduce manufacturing costs, including raw material usage and manual labour.

1. Introduction

Additive Manufacturing (AM) has gained popularity worldwide over the past decades. It is often interchangeable when referring to the AM process with terms of 3D printing, layered manufacturing, rapid prototyping, and rapid manufacturing [1]. AM technology covers many processes in which consumable material is deposited or jointed under the control of certain Computer Aid Manufacturing (CAM), depositing three-dimensional object layer by layer [2]. Recently, the focus of AM has changed to fabricate expensive metal components such as titanium [3] and nickel alloys [4] in the aerospace industry where such components often suffer an extremely high buy-to-fly ratio [5]. Commonly, AM technologies for metallic parts include: i) wire arc additive manufacturing (WAAM); ii) Electron beam freeform fabrication (EBF3); iii) Electron beam melting (EBM); iv) Selective laser sintering (SLS); and

Selective laser melting (SLM) [6]. amongst these, WAAM, which combines electric arc as the power source with welding wire as a feedstock, is able to fabricate large scale parts with high efficiency and low cost.

As shown in Fig. 1, the WAAM process consists of several major processing steps: (i) bead modelling, the relationship between the welding parameters and the bead geometries; (ii) 3D slicing, a 3D model is sliced into a set of 2.5D layers with predetermined thickness; (iii) 2D path planning, the optimal deposition path is designed to fill the 2.5D cross-sections; (iv) deposition process, the welding process parameters are selected according to the weld bead modelling and the molten material is deposited along the path layer upon layer; and (v) post-process machining, the part is machined for removing extra support structure and/or to meet a desired surface quality [7]. In the WAAM process, each layer is deposited with a large number of single weld beads side by side. The offset distance of adjacent beads has a great impact on the geometric

* Corresponding author.

E-mail addresses: dd443@uowmail.edu.au (D. Ding), fh271@uowmail.edu.au (F. He), ly930@uowmail.edu.au (L. Yuan), zengxi@uow.edu.au (Z. Pan), leiw@uow.edu.au (L. Wang), montse@uow.edu.au (M. Ros).

The authors contributed equally to this work.

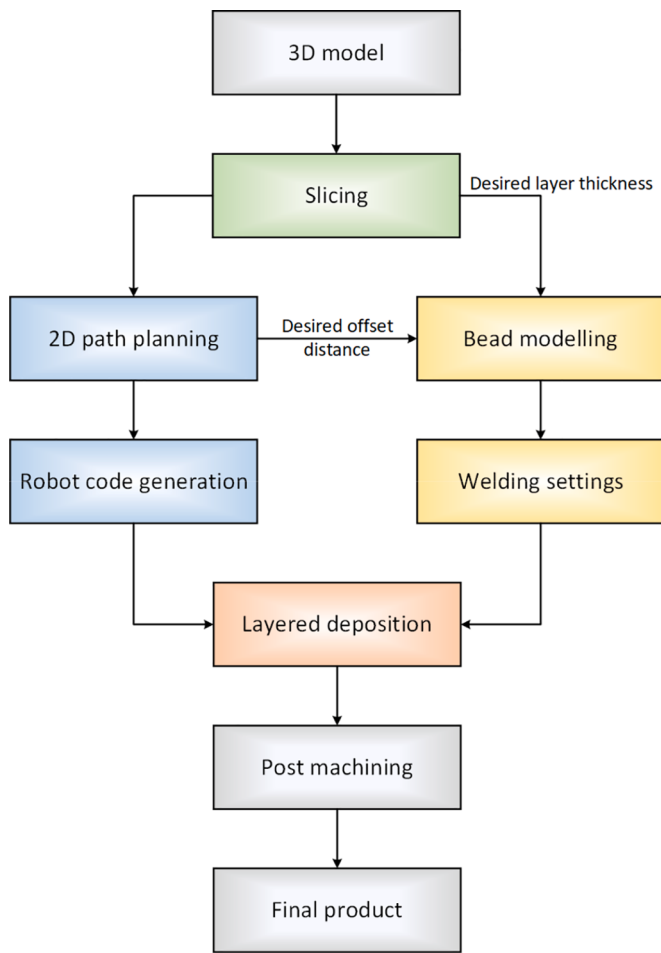


Fig. 1. The steps of the WAAM process.

accuracy and surface quality [5]. Besides, the height of the weld bead, to some extent, is also required to be the same as the layer thickness for 3D slicing. To realize a practical WAAM process, the relationship between weld bead geometry and welding process parameters is critical to select optimal welding process variables. However, for current WAAM systems, the welding variables are still determined manually or partially automated based on a database and operator experience that may affect the accuracy and the efficiency of the WAAM process [8]. For example, in the study by Ding, et al. [7], the authors proposed a fully automated WAAM system, which only requires the 3D profile as system input and creates the final part without human intervention. However, the bead modelling module is only capable of predicting bead geometry with the given welding parameters. Similarly, in the WAAM system proposed by Prado-Cerqueira, et al. [9], the collected experimental results were used as a database to provide information for weld settings. Therefore, it is imperative to develop an automated bead modelling system to achieve an intelligent WAAM process.

Currently, many modelling methods have been proposed for creating a forward model for weld bead formation, such as traditional regression model [10–12], Taguchi approach [13], and Artificial neural networks (ANNs) [14–16]. The forward model is referring to the predictive model that is able to predict the bead geometry based on the given welding parameters. However, it is difficult to produce accurate weld bead geometry with the limited welding parameter sets. This is considered a drawback of the forward model. In practical industrial production, parts may have complex geometries, therefore the weld bead geometries are always required to be varied slightly when fabricating parts with complex structures. Ideally, the weld bead model should be used in reverse, which means the welding parameters can be obtained based on the weld

bead geometry generated in the path planning process. Xiong, et al. [8] used ANNs method to develop both forward and backward model for predicting welding parameters. The backward model is referring to the predictive model that is able to predict the welding parameters based on designated bead geometry. The authors conclude that the accuracy of the backward model is unsatisfactory, and the forward model was used to examine the accuracy of the backward model. If the error between the predicted and desired bead geometry is unacceptable, the welding variables are slightly adjusted for the next iteration until the error becomes smaller than a threshold. Note that the parameters are adjusted based on the influence of welding variables on the bead geometry according to the reference [10].

Compared to conventional ANNs based model, Support vector machines (SVMs), an alternative machine learning algorithm, has the potential to provide a more accurate and efficient solution for the bead modelling process in WAAM. In machine learning, SVMs are supervised learning methods with corresponding learning algorithms that process data used for regression analysis [17]. In many studies, the SVMs are identified to be superior to ANNs, as they avoid some major weaknesses of ANNs: (i) SVMs often converge on global minimum rather than local minimum, which means ANNs model may miss the optimal result [18]. (ii) ANNs has the limitations on generalization giving rise to models that may lead to overfit the data. (iii) The training time of SVMs is substantially less than that of ANNs [19]. In the current literature, SVMs have been demonstrated a good capability of solving regression issues for various applications [20–22]. For the modelling problem in welding, Chen, et al. [23] proposed a modelling method to predict weld penetration using SVMs in gas tungsten arc welding. The experimental results indicate that the SVM-based model shows a higher level of accuracy in predicting welding penetration by comparing with the ANN method. To date, little has been done to create a highly accurate weld bead model for WAAM using SVMs.

This study aims to develop an automated bead modelling system from weld bead deposition, data collection, and processing to welding parameters prediction in WAAM process. Conventionally, the system would be developed by manufacturing engineer. However, knowledge on a single discipline can not meet the industrial requirements of high level of accuracy, product quality, and system automation, the integration of technologies from a number of disciplines should be considered. Industrial information integration engineering is carried out to solve complex industrial problems by combining methods [24]. As comprehensively reviewed in [25,26], industrial information integration engineering is an emerging subject attracting much attention in academia. Moreover, Chen [25] also pointed out that research on the manufacturing category was the second biggest category in this industrial information integration. Thus, the bead modelling system was proposed through integrating information and knowledge from computer science, material engineering, mechanical engineering, and industrial system engineering. As the first step of the WAAM process, the fully automated WAAM system can improve product quality and reduce the time required for the design and manufacturing cycle. In addition, Machine learning is firstly used for weld bead modelling in WAAM process. A novel algorithm using SVM was proposed for the system which provides users with a set of accurate welding parameters for the deposition of weld bead with designate geometry.

In the following sections, the workflow of the proposed system is described in [Section 2](#). In [Section 3](#), the data collection and processing system is presented and the SVMs based modelling algorithm is detailed in [Section 4](#). The effectiveness of the proposed system is examined through the experimental validation and a case study in [Section 5](#), and followed by a conclusion in [Section 6](#).

2. System overview

This paper proposes a novel Computer Aided Manufacturing (CAM) system for bead modelling process using arc welding-based AM

technology. Weld beads are deposited side by side, as demonstrated in Fig. 2, the sliced layer height and offset distance are the same as the desired bead high (BH) and overlapping distance (OD). Thus, the proposed system aims to generate optimal welding parameters and setups to produce the user preferred bead geometry.

2.1. The operation procedure

The overall workflow of an automated bead modelling process for WAAM system is presented in Fig. 3. It consists of three essential modules including, data generation, model creation, and welding parameter generation. All three modules will be called step-by-step when the weld bead model for the selected operation welding mode and filler material does not exist in the current model library. This is because the weld bead morphology indicates that the weld bead geometry is different with varied welding methods and filler materials. Consequently, a new bead model is required to be created. Otherwise, only the welding parameter generation module will be called. The detailed workflow of the system is described as follows:

The Data generation module is used to provide data for model creation, in which four steps are included from depositing weld beads to obtaining bead geometry information. Firstly, the welding setup, including the range of welding parameters, the length of a single bead, the substrate plate dimensions, etc., are required as user inputs for the system. Secondly, according to the welding setup, an optimal deposition plan for the bead on plate process are provided by the developed software and the bead on plate process can be executed automatically. In this step, the user only needs to place the base plate to the predetermined location and trigger the deposition. Thirdly, the bead profiles are scanned by the laser scanner and the data are recorded. Finally, the raw data of the bead profiles are processed to generate the bead height and optimal overlapping distance with their welding parameters for model creation.

The Model creation module builds bead models based on the obtained data. An SVM algorithm is used to build up the relationship between

welding parameters and bead geometries. The detailed algorithm of the SVMs based modelling process is presented in Section 4. Once a model is created, it will be saved and labelled in the model library for the next module.

The Welding parameter generation module is used to provide the optimal welding process parameters for the deposition process. Firstly, the correct model is selected according to the welding method and the filler material. Then, a set of combinations of welding variables for producing the optimal bead geometries can be generated. In an arc-welding based process, the optimal interpass temperature (IPT) can effectively help reduce the porosity [27], retain a stable deposition process [28], improve the microstructure and mechanical properties [29]. Thus, researchers would like to select an optimal IPT for the deposition. Meanwhile, the IPT reacts on the molten pool geometry via the thermal boundary condition of the molten pool. It should be mentioned that maintaining a relatively consistent IPT is effective for a better deposition. In the proposed WAAM system, the IPT is controlled by cooling and heating devices so that the workpiece reaches a certain IPT before further deposition. Note that the designation of IPT is not compulsory. If the IPT is not selected, since the temperature is also an input factor for bead modelling, the developed bead modelling can generate the optimal process parameters including temperature (IPT). If the user designates the IPT range, the system is able to search the most accurate welding parameters with IPT in the selected range.

2.2. The hardware of the system

The basic hardware of the automated bead modelling system includes an industrial robot, a worktable, a welding machine, a computer, an infrared pyrometer, and a laser scanner. Fig. 4 displays the hardware setup for this study. An ABB IRB 2600 industrial robot with six Degrees of Freedom (DoF) is used to hold and move the welding torch along the preprogrammed deposition path. The welding power source is a Fronius CMT Advanced 4000 welding machine with a number of GMAW based

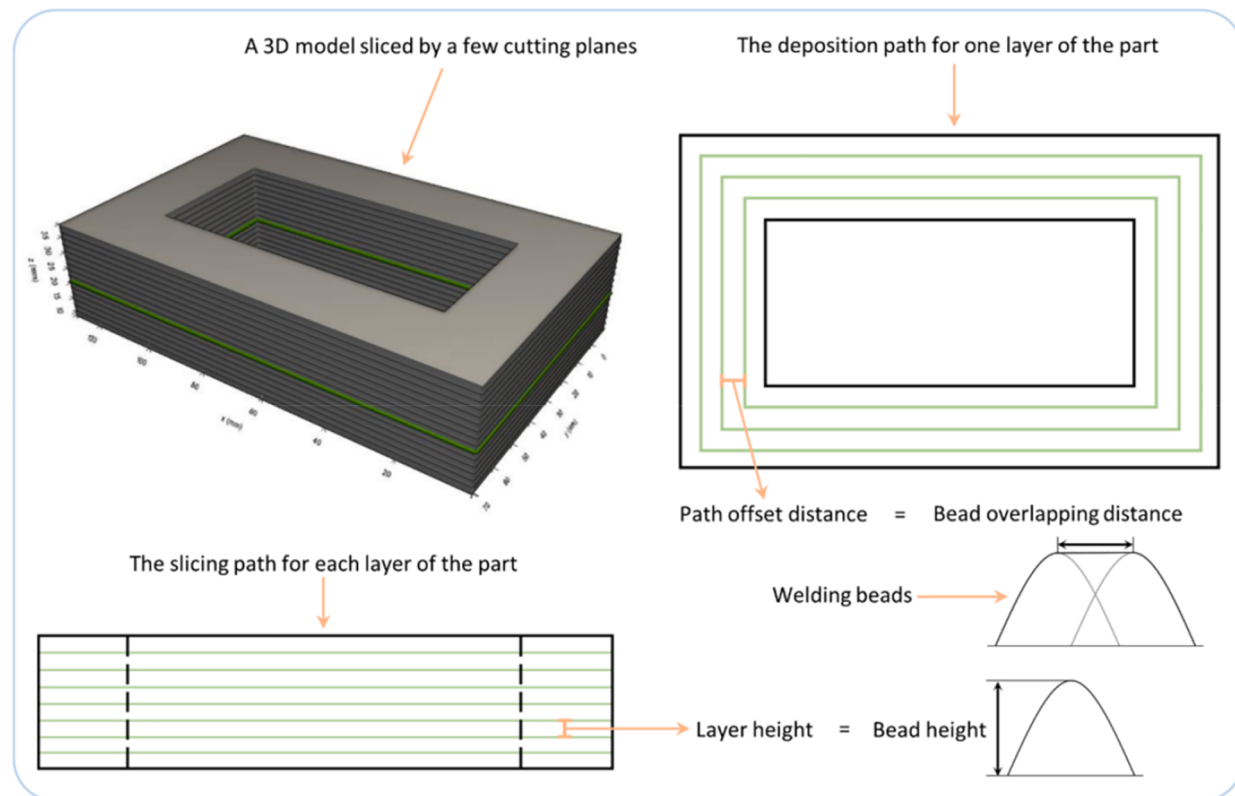


Fig. 2. The requirement of overlapping distance and bead height in path planning process.

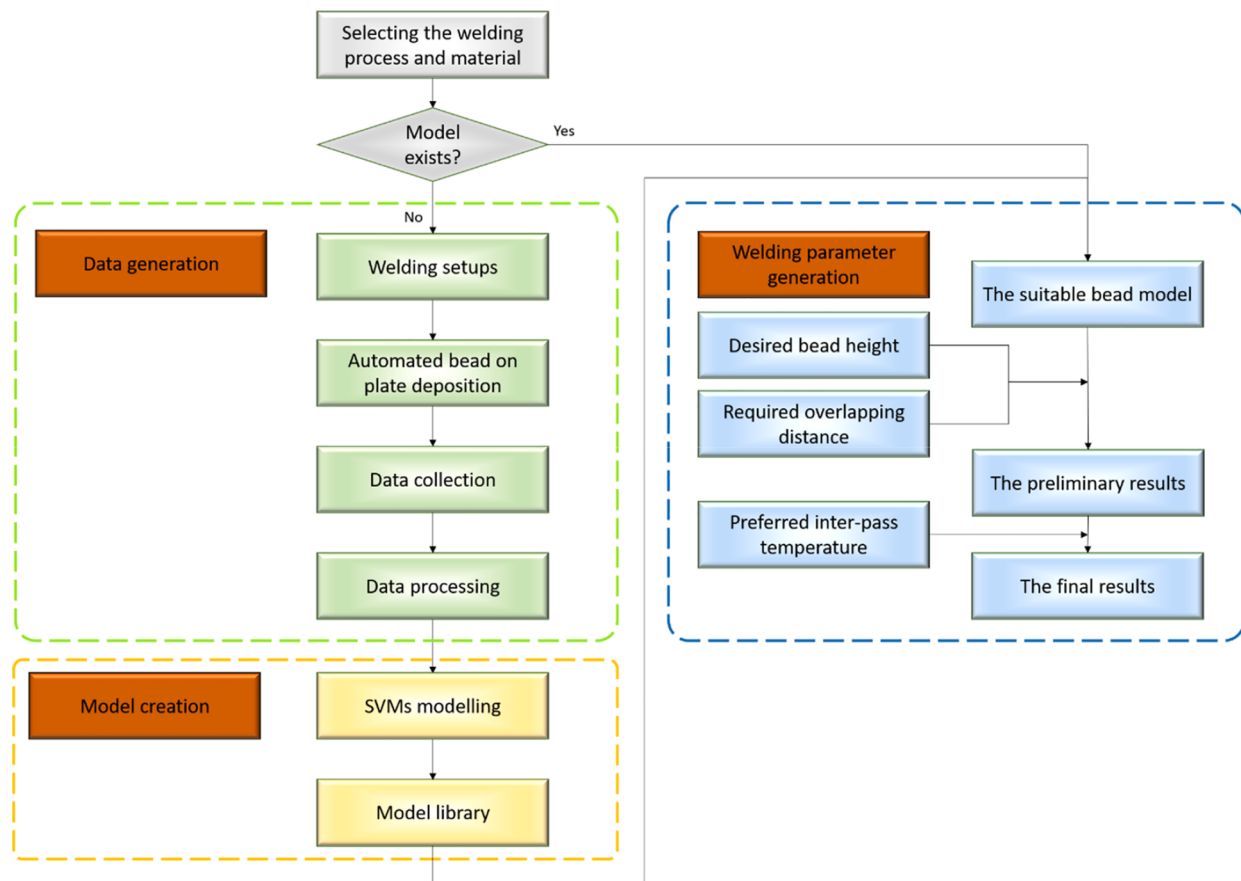


Fig. 3. The steps of an automated bead modelling process.

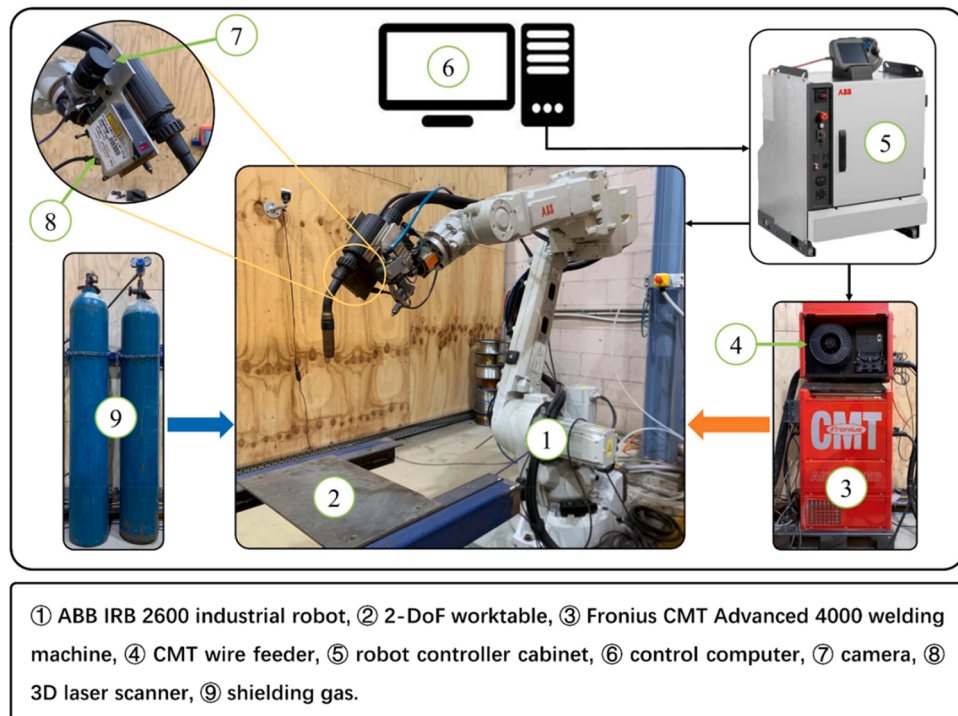


Fig. 4. The experimental setup of the WAAM system.

welding modes to select from. Robot Studio (simulation and programming software for the ABB robot) was used to program the torch motion and coordinate the weld settings. The base plate is placed on a 2-DoF worktable, note that the position of the worktable is fixed and calibrated carefully to ensure an accurate weld bead position for scanning. A structured light laser scanner is integrated into the robotic welding system to measure the bead profile. An infrared pyrometer was used to monitor the inter-pass temperature. A data acquisition unit and a personal computer serve as the master control for the welding machine, robot, laser scanner, and infrared pyrometer.

2.3. Software and user's graphical interface

Based on the presented workflow in Section 2.1, software has been developed for a non-expert operator to monitor and control the bead modelling process, the user-friendly interface is shown in Fig. 5. The programming language Python was used to develop the software. Five steps are included as described below.

Step 1, model selection: firstly, the users are required to select an application type between the thin-walled structure and the solid structure. Then, the welding method and filler material should be selected to check if the bead model for the selected welding process exists. If it is positive, welding parameters generation model will be loaded, and the welding parameters can be generated directly. Otherwise, if the model does not exist, a new model can be saved and named with the welding method and filler material.

Step 2, bead on plate deposition: in this step, the information of the welding setups is required for the bead on plate deposition, including welding parameters range (Wire Feed Speed (WFS), Travel Speed of the torch (TS), and Inter-Pass Temperature (IPT)), and dimensions of the

base plate. With the inputs, a preview image of the distribution of weld beads on plate process is shown. More detailed information, the total number of weld beads and base plate, length of each weld bead, and offset distance of the adjacent bead, are provided automatically.

Step 3, deposition control: this step is used to monitor and control the bead deposition and data collection process. Once the operator places the plate on the working table, the entire deposition and data collection process will be executed automatically.

Step 4, data processing and bead modelling: the OD and BH of each weld bead can be generated by processing the raw data of the weld bead profile. Then, the bead model is trained using the SVM based algorithm and it is saved to the model library in the system.

Step 5, welding parameter generation: Once a new model is exported to the library for a specific welding task, the user can obtain the optimized welding parameters by inputting the required OD, BH, and IPT.

3. Data collection and processing

Generally, the bead modelling process identifies the relationship between weld settings and bead profiles. The data generation module is used to provide essential weld bead geometry data for creating the weld bead model. The module includes three major steps, bead on plate deposition, data collection, and data processing.

3.1. Bead on plate deposition and data collection

Firstly, a set of weld beads are deposited with the designated welding parameters. According to the dimensions of the base plate, the length of each bead is 100 mm. The distances between adjacent beads and columns are set to 30 mm and 40 mm. The detailed arrangement of bead

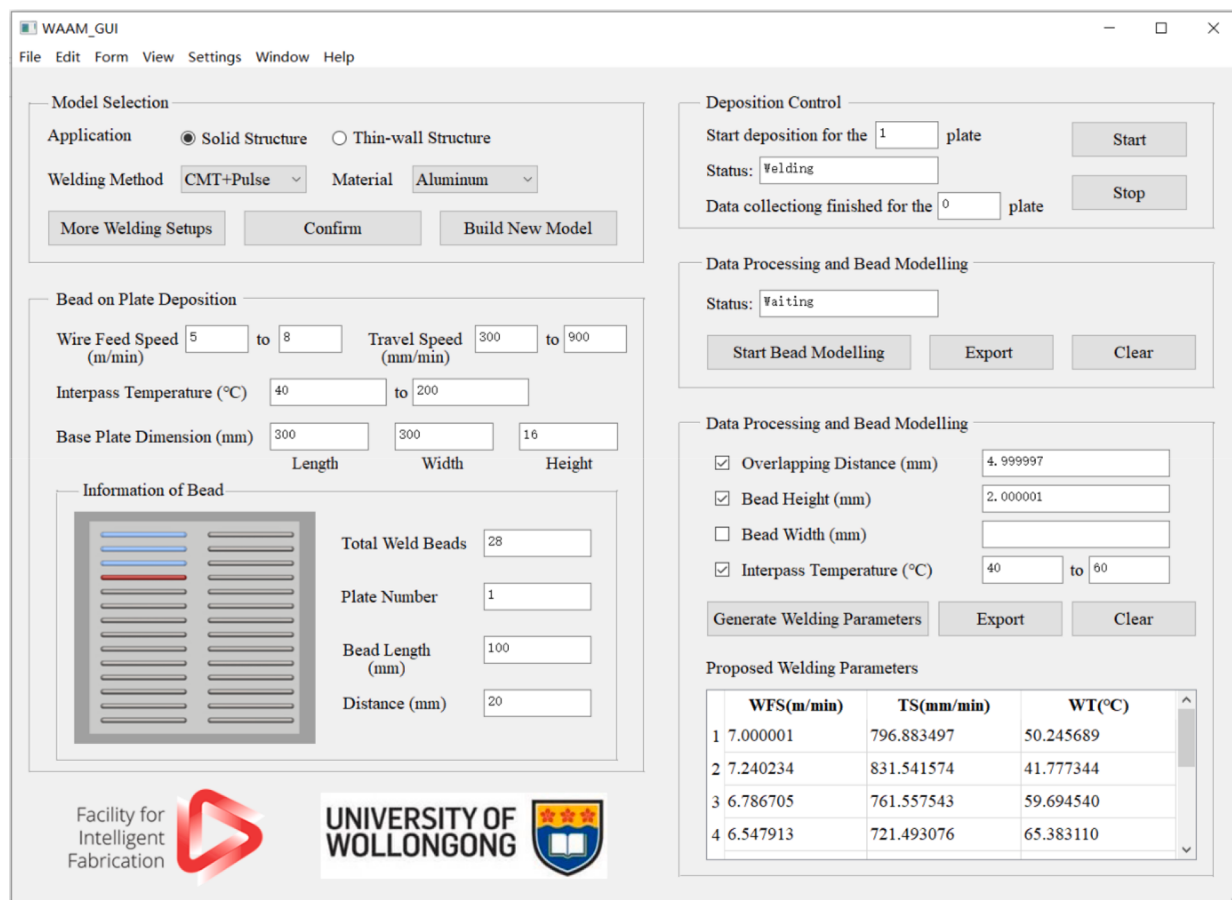


Fig. 5. WAAM rapid bead modelling graphical user interface.

locations is presented in Fig. 5. In the deposition process, movements of the welding torch are automatically programmed in the robot controller. The welding parameters, such as WFS and TS, are automatically set to the designated values for each deposit. It is worth mentioning that a IPT control system is used in the modelling process, a thermal pyrometer is used to monitor the IPT. A ceramic heater pad and compressed air nozzle are applied to heat up or cool down the base plate to the designate IPT. A laser scanner is used to measure the profile of beads, as illustrated in Fig. 6. It scans the weld beads along the weld path and records the transverse bead profile of each weld bead.

While for the thin-walled structure, data collection is quite different from that for the solid structure. In order to collect effective bead geometry for machine learning, single-pass multi-layer (normally four layers) beads were deposited layer-upon-layer rather than the single bead-on-plate. In this scenario, only the geometry of the fourth bead will be scanned and recorded for model creation. It worth mentioning that the profile of the third layer will be scanned before the fourth layer deposition so that the bead height and width can be calculated by comparing the differences between the third and the fourth layer. If a significant difference in bead width and height were observed, the fifth layer deposition is required. Until the uniform bead geometries between the successive layers are achieved, the data will be processed.

3.2. Data processing

The target of the data processing is to obtain the OD and BH through the raw data of weld bead profile. In order to depict the geometry of weld beads accurately, a data processing algorithm was proposed. It includes: (i) a signal denoising filter, (ii) bead profile extraction, (iii) curve fitting process, and (iv) generation of the OD and BH.

Step 1, signal denoising. As noise is inevitably recorded by the laser scanner, a moving average filter is used for smoothing raw data. The moving average filter is a type of low pass finite impulse response filter (LPF) which can be used for regulating an array of sampled data. The LPF uses Hamming window with the sampling frequency and cut-off frequency were set to 10,000 Hz and 400 Hz respectively. Most of the noise points in the data set are removed after filtering. The processed data after denoising is presented in Fig. 7(a).

Step 2, bead profile extraction. As a number of weld beads are scanned simultaneously by the laser scanner as shown in Fig. 7(a), a

boundary detection program was developed to extract single bead profile in each data set. Firstly, the boundaries of each weld bead are identified by calculating the change rate of slope in the y-axis. Points between the left and right boundary are saved to represent the weld bead profiles, as shown in Fig. 7(b).

Step 3, curve fitting process. To obtain OD and BH accurately, accurate weld bead profiles are required. Thus, the weld bead profile data from the laser scanner needs to be further processed. Commonly, various functions are used to fit the cross-section of the weld bead. In the research by Xiong, et al. [30], the parabola, arc, and cosine functions can be applied to build the profile of the weld bead. In our previous study [5], a number of curve fitting methods were used to create bead profile models. Through the comparison of the developed model, the experimental results reveal both parabola and cosine functions accurately represent the bead profile. In present study, the parabola function was chosen to fit the cross-section of weld bead. The fitted parabola function can be represented by

$$y_1 = ax^2 + c \quad (1)$$

Step 4, generation of the bead overlapping distance. In the practical deposition process, the BH and OD are used to determine the layer height and offset distance between adjacent weld path. The BH can be obtained by searching the vertex coordinates of each parabolas function directly. In the literature, the overlapping distance, d , between adjacent beads plays an important role in determining surface quality and smoothness. Fig. 8(a)-(c) illustrate the principle of generating OD using the tangent overlapping model (TOM) [5]. As the overlapping distance is decreased, the overlapping area increases, and the area of the valley decreases. The overlapped surface observed during a large amount-number of welding tests can be depicted as a tangent line with the second bead. When the valley area (S_1) is equal to the overlapping area (S_2), the critical state is reached.

As described in Fig. 8(a), two identical welding beads are deposited next to each other with the offset distance d . Based on the polynomial fitting result in Step 3, the parabola function which can represent the adjacent bead profile is shown as below

$$y_2 = a(x - d)^2 + c \quad (2)$$

where c is equal to the weld height h and $a = -4h/w^2$. To generate a flat

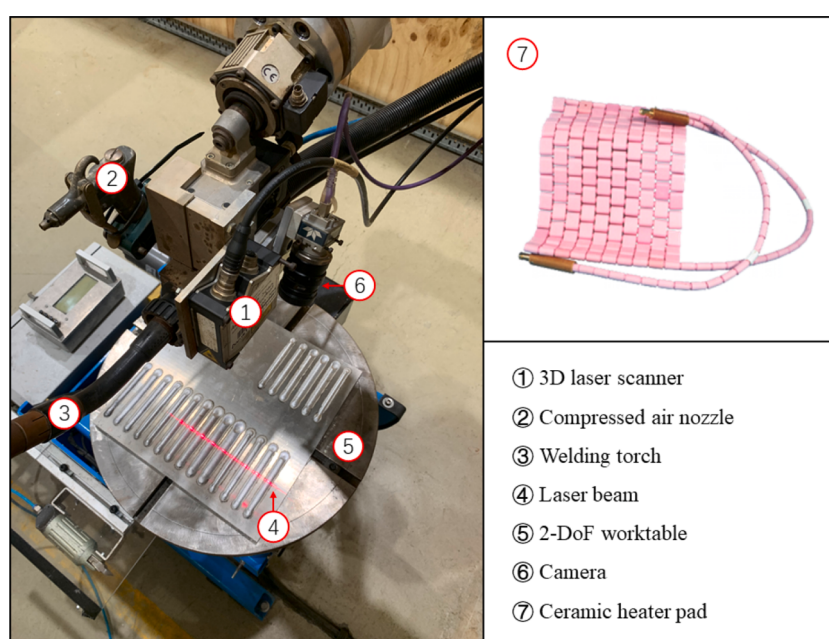


Fig. 6. Weld bead profiles collection using the laser scanner.

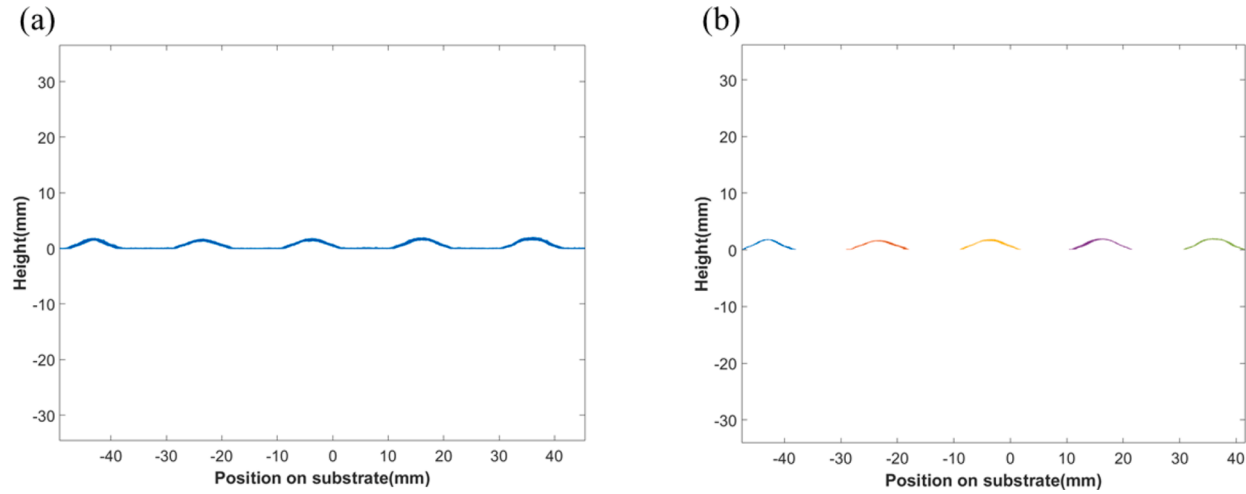


Fig. 7. Bead profile denoise and extraction.

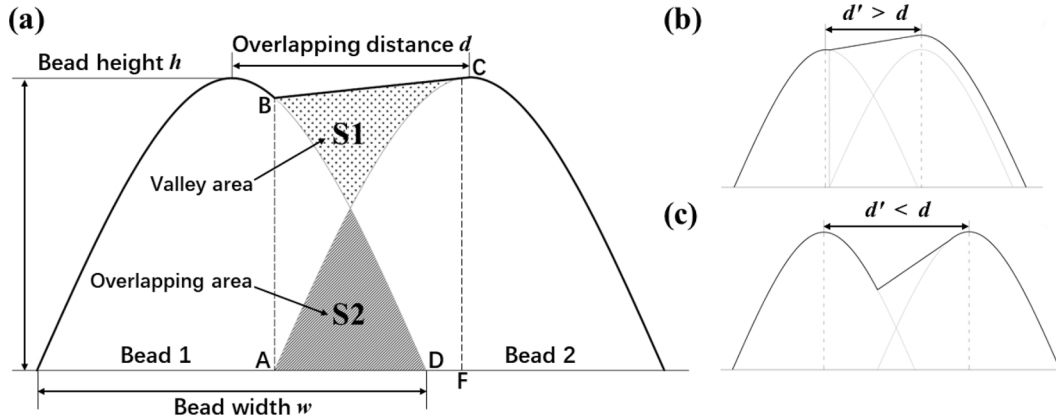


Fig. 8. Schematic diagrams of the tangent overlapping model (TOM).

layer surface, an optimal value of $d = d'$ should be selected so that the critical valley area S_1 equals to the overlapping area S_2 . If the coordinates of points A, B, F and C are defined as $A(x_1, 0)$, $B(x_1, y_1)$, $F(x_2, 0)$ and $C(x_2, y_2)$, then S_1 and S_2 can be calculated as

$$S_1 = \frac{y_1 + y_2}{2}(x_2 - x_1) \\ + 2 \int_{x_1}^{d/2} (ax^2 + c)dx \\ - \int_{x_1}^{\sqrt{-c/a}} (ax^2 + c)dx \quad (3)$$

$$- \int_{x_1}^{x_2} [a(x - d)^2 + c]dx \\ - \int_{x_1}^{x_2} [a(x - d)^2 + c]dx \quad (4)$$

We define $f(d)$ as the function of the difference between S_1 and S_2 :

$$f(d) = S_1 - S_2 = \frac{1}{3}ad^3 + \frac{1}{6}aw^3 - \frac{1}{2}awd^2 \\ - \frac{ad(w-d)}{3}\sqrt{wd-d^2} \quad (5)$$

When $S_1 = S_2$, $f(d) = 0$. amongst the four roots obtained from this equation, only two of them have positive real values:

$$d_1 = w \quad (6)$$

$$d_2 = \\ w \left[\left(\sqrt{\frac{1}{512}} + \frac{1}{16} \right)^{1/3} + \frac{1}{8} \left(\sqrt{\frac{1}{512}} + \frac{1}{16} \right)^{-1/3} \right] \\ \approx 0.738w \quad (7)$$

This indicates that S_1 is equal to S_2 when the offset distance d is equal to the critical centre distance $0.738w$.

Since the TOM was verified experimentally and was widely accepted in the field of WAAM, it is adopted in this paper. For more detailed information about the tangent overlapping model, refer to the reference [5]. Finally, d' will be recorded into the library as the OD for the selected weld bead profile. A set of ODs and BHs with their corresponding welding parameters will be sent to model creation process.

4. Modelling of the weld bead

This section includes the model building process and parameter prediction process. The purpose of this modelling process is to generate a model that can represent the relationship between welding parameters and bead profile parameters, and furthermore, is to provide the welding parameters that meet the path planning state requirements, as discussed

in Section 2. Therefore, a successful model should be able to predict the welding parameters by the given bead profile parameters which are OD and BH in this case.

To generate the bead model under various WFS, TS, and Temperature, the values of the chosen process variables at various levels are listed in Table 1. A total of around 60,000 effective weld bead profiles from the 200 deposited weld beads were processed for machine learning. There were 500 transverse sections of profiles recorded for each weld bead, which means the bead profiles were recorded for every 0.2 mm since the length of each weld bead is 100 mm. Only the 300 profiles of weld bead in the middle will be processed due to the unstable deposition during arc on/off. In addition, irregular profiles were deleted and the rest profiles were extracted for further processing. Note that the bead data under the current welding parameters will be excluded if the effective bead profiles were less than 200.

This section mainly contains an overview of the whole modelling process, and the details of the modelling process by using three different machine learning algorithms. Note that the description in this section was based on the modelling process for a solid structure. For thin-walled structures, OD can be replaced by bead width (BW).

4.1. Forward model

The forward model is referring to the predictive model that is able to predict the bead profile based on the given welding parameters. This subsection includes the detail of the modelling process by using the Support Vector Regression (SVR) method.

4.1.1. Support vector regression method

SVMs can be used for multiple tasks in data analysing such as novelty detection, classification and regression analysis while SVR can be considered as a variant of SVMs, which is particularly used for solving regression problems.

The basic theory of kernel-based SVR is to implicitly map the input variable x onto a higher dimensional feature space via function Φ and perform nonlinear mapping in the feature space [31]. Instead of calculating the inner product, the complex calculations in the high dimensional feature space can be completed by using a kernel function [32].

Considering a given set of training data $\{(x_1, y_1), (x_2, y_2), \dots, (x_n, y_n)\}$, where $x_i \in R^N$, $y_i \in R$, $i = 1, 2, \dots, n$, where n corresponds to the size of training data, the regression model can be estimated by introducing a general function shown below

$$f(x) = (w \cdot \Phi(x)) + b \quad (8)$$

where w , b denotes the weight vector and threshold value respectively and Φ is a nonlinear transformation from R^N to a high dimensional feature space. When ϵ is used as the insensitive function, the SVR can be considered as ϵ -SVR which takes the form

$$|y - (w \cdot \Phi(x) + b)| = \begin{cases} 0 & |y_i - (w \cdot \Phi(x) + b)| < \epsilon \\ |y_i - (w \cdot \Phi(x) + b)| - \epsilon & |y_i - (w \cdot \Phi(x) + b)| > \epsilon \end{cases} \quad (9)$$

Table 1
Process parameters for machine learning.

Parameters	Factor levels						
	Level 1	Level 2	Level 3	Level 4	Level 5	Level 6	Level 7
WFS (m/min)	5.0	5.5	6.0	6.5	7.0	7.5	8.0
TS (mm/min)	300	400	500	600	700	800	900
IPT (°C)	40	80	120	160	300		

where ϵ is a positive constant. This function shows that the model will ignore the fitting errors that are less than ϵ , which increases the anti-noise ability of the regression model [33].

In order to find the value of w and b , it is necessary to measure the deviation degree based on the ϵ insensitive band of training data. Therefore, two non-negative relaxation factors ξ and ξ^* have been employed. The SVR optimization model can be represented as follows

$$\min_{w,b,\xi,\xi^*} \frac{1}{2} w^2 + C \sum_{i=1}^n (\xi_i + \xi_i^*) \quad (10)$$

The formula above has several constrain conditions

$$\min_{w,b,\xi,\xi^*} \frac{1}{2} w^2 + C \sum_{i=1}^n (\xi_i + \xi_i^*) \quad (11)$$

$$y_i - f(x_i) \leq \epsilon + \xi_i^*, \quad i = 1, 2, \dots, n \quad (12)$$

$$\xi_i \geq 0, \xi_i^* \geq 0, \quad i = 1, 2, \dots, n \quad (13)$$

The element of $C \sum_{i=1}^n (\xi_i + \xi_i^*)$ represents the deviation between $f(x_i)$ and y_i . When $f(x_i)$ and y_i have totally equal value, the loss error will become zero. The constant C denotes the error penalty factor, which can modify the complexity and loss error.

A Lagrange function has been introduced for the SVR optimization and a dual optimization formula can be obtained as follows

$$\begin{aligned} \min_{w,b,\xi,\xi^*} L(w, b, \alpha^*, \xi, \xi^*, \mu, \mu^*) \\ = \min_{w,b,\xi,\xi^*} \frac{1}{2} w^2 + C \sum_{i=1}^n (\xi_i + \xi_i^*) \\ - \sum_{i=1}^n (\mu_i \xi_i + \mu_i^* \xi_i^*) \\ + \sum_{i=1}^n \alpha_i (f(x_i) - y_i - \epsilon - \xi_i) \\ + \sum_{i=1}^n \alpha_i^* (y_i - f(x_i) - \epsilon - \xi_i^*) \end{aligned} \quad (14)$$

After solving the above dual formula by making the partial derivative of w , b , ξ , ξ^* equal to zero, the mathematical expression of SVR model can be obtained

$$f(x_i) = \sum_{i=1}^n (\alpha_i - \alpha_i^*) K(x_i, x) + b \quad (15)$$

where

$$b = y_i + \epsilon - \sum_{i=1}^n (\alpha_i^* - \alpha_i) K(x_i, x) \quad (16)$$

The $K(x_i, x)$ is the kernel function and α_i , α_i^* are the Lagrange multipliers. The data samples which correspond to the non-zero part of α_i , α_i^* are defined as support vectors (SV).

Kernel function enables the implementation of inner products in a high dimensional feature space by using the original input data without the need to know the transformation function Φ . The previous studies [34,35] showed that the model using Gaussian radial basis function kernel (RBF) can usually perform regression estimation accurately and efficiently. Therefore, the RBF kernel has been implemented in the SVR model in this work. This kernel function can be represented as follow

$$K(x_i, x_j) = \exp\left(-\frac{\|x_i - x_j\|^2}{\sigma^2}\right) \quad (17)$$

where σ can decide the radial range of the function. The LIBSVM library [31] transforms the formula into a more concise form

$$K(x_i, x_j) = \exp\left(-\gamma||x_i - x_j||^2\right), \gamma > 0 \quad (18)$$

where $\gamma = \sigma^{-2}$.

4.1.2. k-fold cross-validation

According to the mathematical expression of the SVR model and the RBF kernel, selecting the appropriate value of C and γ is very important to the regression estimation. These hyperparameters in the SVR model could be empirically set. However, this makes the hyperparameter values highly dependant on human experiences, and their optimality cannot be guaranteed under this circumstance. Hence, researchers have proposed advanced parameter optimization methods, such as mesh search algorithm, leave one out (LOO) error evaluation, and so on. Also, some search algorithms were proposed to be used in parameter adjustment, such as gradient descent algorithm, genetic algorithm, and so on. The k-fold cross-validation algorithm is one of the most commonly used method for efficient model validation and statistical analysis.

The LIBSVM has provided a k-fold cross-validation function which allows user to input the training data set and (C, γ) values that need to be tested. It will output Mean Square Error (MSE) corresponding to each group of (C, γ) [36].

As described in Fig. 9, the basic idea of the k-fold cross-validation algorithm is to firstly divide the training data set into k groups $\{\alpha_1, \alpha_2, \dots, \alpha_k\}$ and each group has the same number of the data samples. At first, group α_1 is used as the test set, and the rest groups are jointly used as the training set to train the SVR model with certain (C, γ) . Once the model is trained, the LIBSVM function will output the corresponding MSE on group α_1 as the evaluation of the model. The above procedure will be repeated by using each group α_i as the test group and the rest groups as

the training group in turn. After k iterations, k groups of MSEs will be generated. The average of MSE (AMSE) can be obtained by using the formula

$$AMSE = \frac{\sum_{i=1}^k MSE_i}{k} \quad (19)$$

After conducting the k-fold cross-validation, each (C, γ) will have a corresponding AMSE. By comparing this value, the most suitable (C, γ) can be obtained. In this modelling process, the value of k has been selected as 5 because of the high efficiency and adequate accuracy [37].

4.1.3. Forward model evaluation

The data set generated in Chapter 3 were used to train and test the forward SVR models. Forward predictive models have been trained and built in order to predict the value of OD and BH at the same time. In other words, these models are aiming to predict the value of OD and BH, respectively, based on the three input parameters WFS, TS and IPT. The most suitable (C, γ) of the models has been found by using the k-fold cross-validation. The model parameters and predicting accuracies are presented in the Table 2.

The comparison between the ground truth value and the predicted value of OD and BH are shown in Fig. 10(a) and (b). In this figure, the group of red line represents the ground truth vale while the group of the green line indicates the predicted value. The diagrams show that the predicted values are highly correlated with the ground truth values.

Table 2
Information of the forward predictive model.

Predicted parameter	C	γ	MSE
Overlapping Distance	8	0.1250	0.0687
Bead Height	524,288	0.0039	0.0077

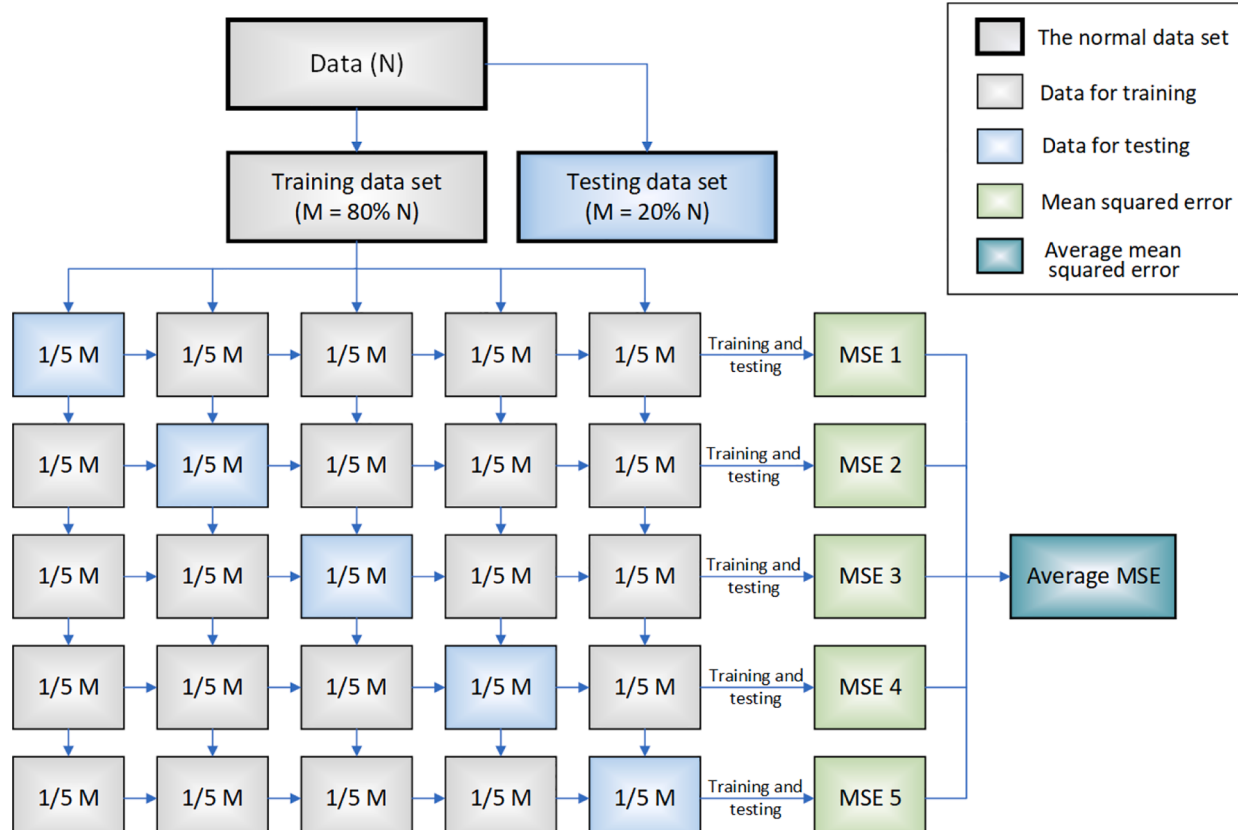


Fig. 9. The basic process of the k-fold cross-validation algorithm.

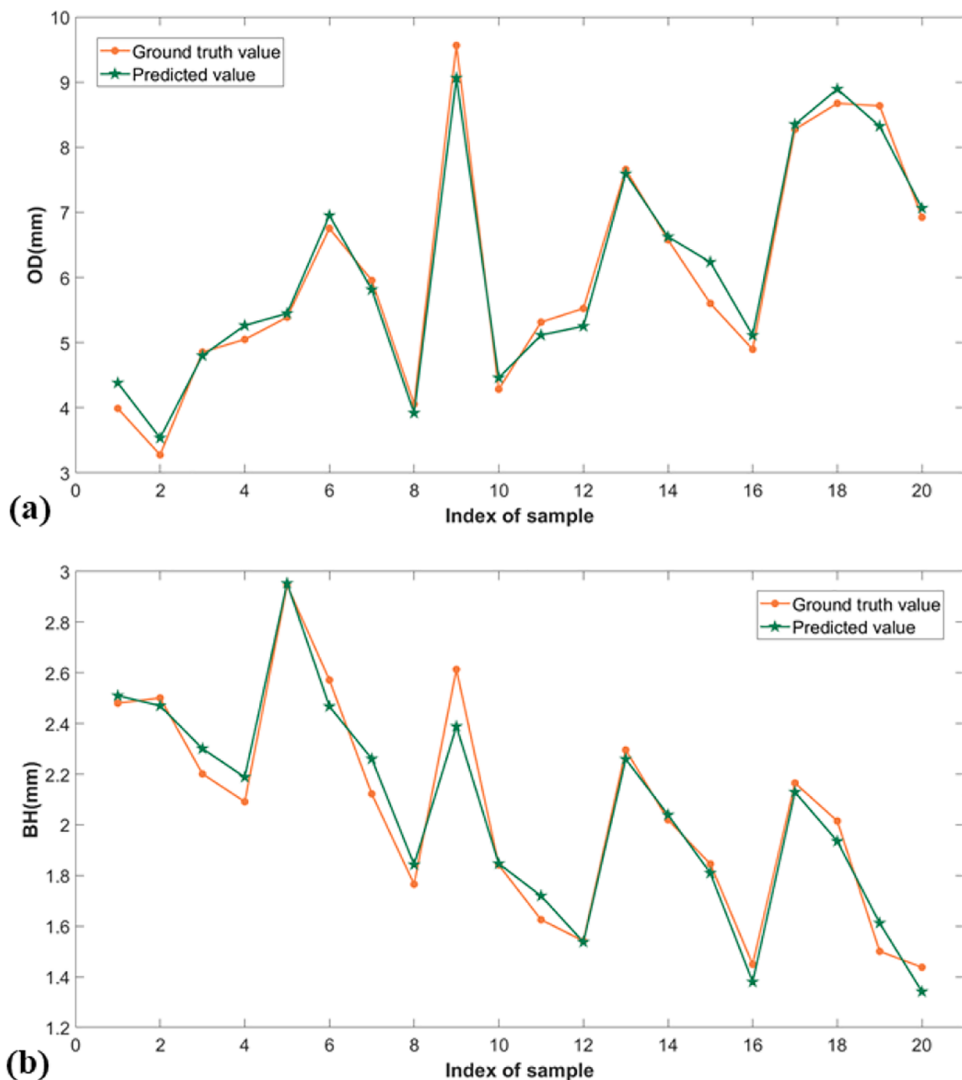


Fig. 10. The comparison between ground truth value and predicted value.

Through all the experiment and modelling process, we have shown that the program used for analysing data also worked well and by using this program, the desired parameters can be obtained accurately and effectively. Finally, a forward regression model with adequate accuracy has been built successfully by applying SVM algorithms. The good performance of the forward predictive model makes it possible to establish a backward model with adequate accuracy and efficiency.

4.2. Backward model

The backward model is referring to the predictive model that is able to predict the welding parameters based on designated bead geometry. Although lots of studies [38–40] mentioned the method to predict the welding bead geometry and also achieved acceptable accuracies, there is currently no opportune backward model for forecasting the welding parameters by expected bead geometry, which has practical significance in industrial manufacturing. The backward model cannot be established by simply reusing the forward predictive model due to the dimension difference between the input and output parameters. The fact that the dimension of input parameters is lower than the dimension of output parameters leads to the accuracy of the backward model on both training and testing sets are not satisfactory [8]. The generalization ability and the approximating nonlinear mappings capacity of which are limited. The results can be attributed to the fact that many combinations

of welding parameters may produce the identical bead geometry. To address this situation, a closed-loop iteration system, consisting of the backward and forward model, was designed for prediction of welding parameters based on the given bead geometry. The main structure of this system is described in Fig. 11.

Because of the data dimension limitation mentioned before, we have to train and build models separately for predicting the three welding parameters. In order to improve the accuracy of the backward model, it is necessary to complete the feature selection of the data before training and building several redundant models. Feature selection refers to the process where we automatically select those features which contribute most to the prediction variable in which we are interested in [41]. In this case, as shown in Fig. 11, for each backward model, we are only interested in the relationship between (OD, BH) and one of the three welding parameters so that the data pieces with one welding parameter as a variable while the other two welding parameters as an integer were selected to train and build an SVR regression model. After this step, a significant number of backward models will be built with different (C, γ). From this procedure, we can see that the 2-dimension inputs and 3-dimension outputs problem has been transformed into 2-dimension inputs and 1-dimension outputs problem, which can be addressed by simply apply SVR algorithm. Then, the desired OD and BH was input to those models as two input variables and from the output of the backward models, a significant number of solutions can be obtained. Obviously,

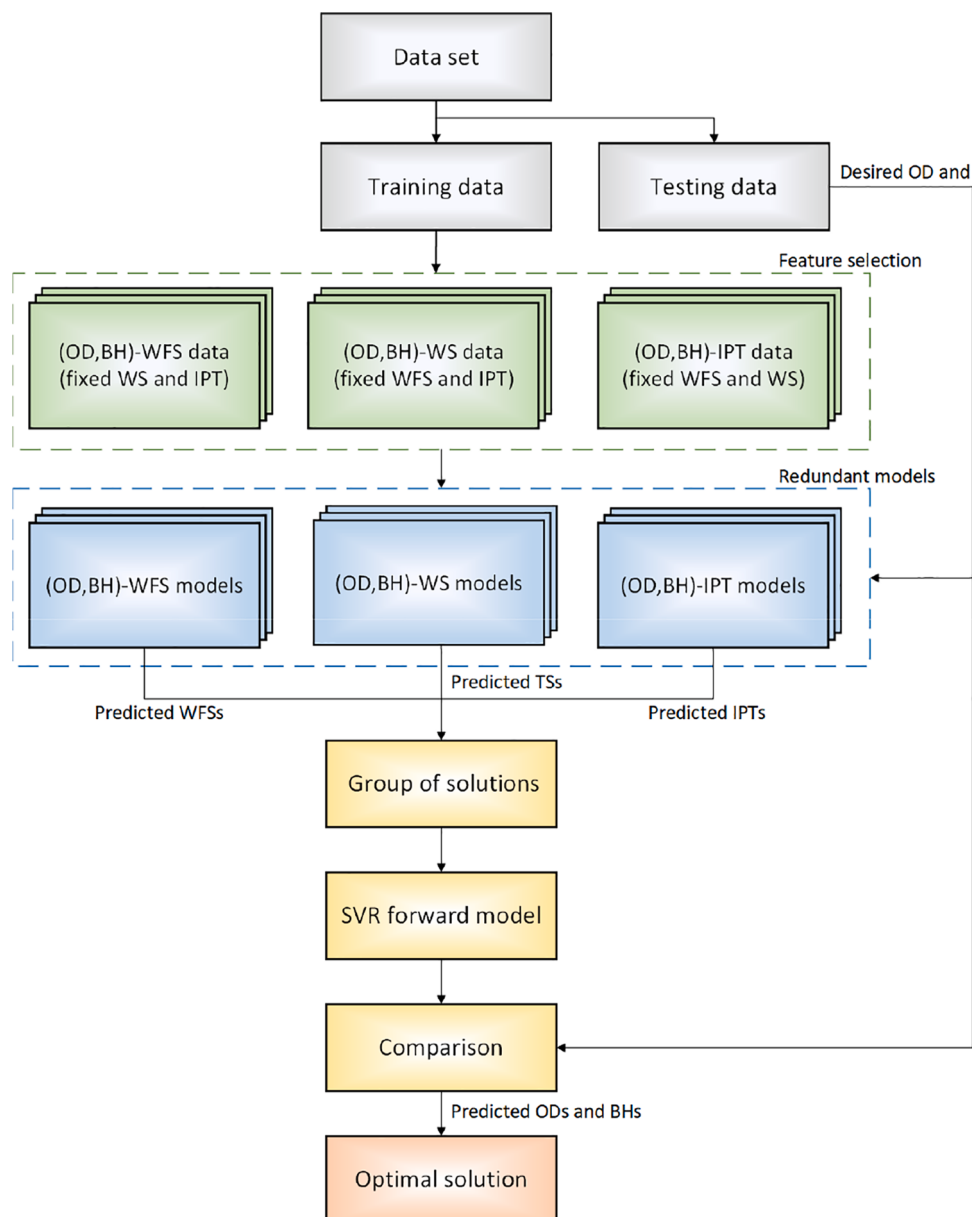


Fig. 11. SVR backward model working process.

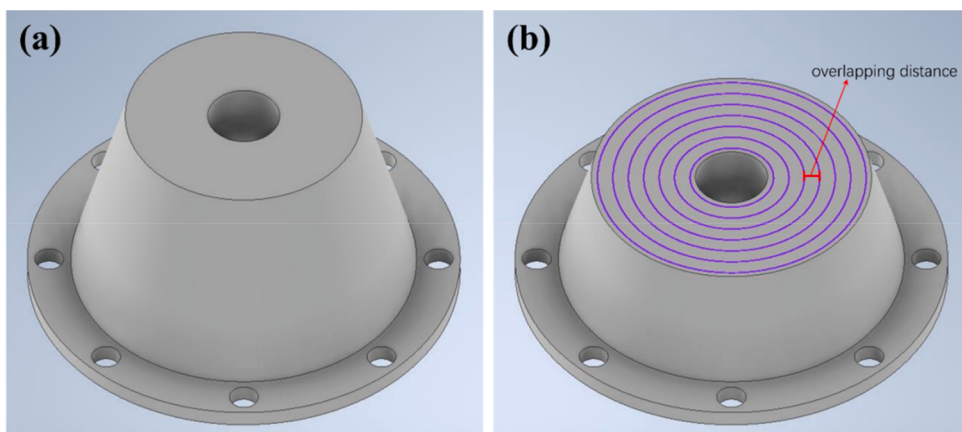


Fig. 12. (a) 3D model of the part, (b) Transverse section of the 21st layer.

many of those solutions are redundant, which means they do not have sufficient accuracy because they are produced by the wrong models. In order to filter out the most accurate solution, all the solutions are input to the SVR forward model as three input variables. Then, after comparing the value of (OD, BH) produced based on predicted solutions and the value of desired (OD, BH), the optimal solution will be filtered out. The problem that using 2-dimension input parameters to predict 3-dimension output parameters has been addressed at the expense of computer memory.

5. Experimental validation and discussion

The performance of the proposed algorithm and system was evaluated through the fabrication of a real-world workpiece, whose 3D model is shown in Fig. 12(a). The detailed fabrication process and relevant discussion are provided in this section.

5.1. Case study

In this case study, the raw material was aluminium 4043 and CMT-pulse welding method. The first step is to slice the 3D model into 39 layers including 3 base layers and 36 body layers (with the predetermined 2 mm layer height). As the 3D model illustrated in Fig. 12(a), the shape of each layer is a ‘doughnut’ with a changing diameter. As shown in Fig. 12(b), the welding torch will move circularly to fill each layer with a number of weld beads. Thus, the overlapping distance of each weld bead varies for adjacent layers.

To generate the near-net shape of the part, the welding parameters have to be constantly adjusted for each layer. However, it is difficult for the conventional bead modelling method to generate accurate welding parameters for all layers. As shown in Fig. 13(a), layers will be divided into a few groups and the same set of welding parameters will be selected to fabricate the target part. The large amount of overbuild volume results in increased manufacturing cost of the WAAM process. Using the proposed SVR based method, the optimal welding parameters can be generated automatically for each layer, aimed at forming a desired geometry of each layer and reducing the overbuild volume, as illustrated in Fig. 13(b).

After slicing the part, the 3D model of each layer was taken out for path planning. Based on the outer diameter of each layer, the number of paths and OD for each layer was determined, targeted at minimizing the overbuild volume. Table 3 presents the calculated OD for each layer. The information about OD and layer height was input to the proposed SVR system. As presented in Table 3, a set of welding process parameters can be obtained by our software.

The deposition process is illustrated in Fig. 14(a)-(d), the outside and

Table 3
The manufacturing information of case study.

Material	Wire diameter 1.2 mm		Shielding gas Pure argon		Flow rate 20 L/min
	aluminum	4043	Input parameters	Predicted welding parameters	
Layer No.	Overlapping Distance (mm)	Height (mm)	WFS (m/min)	TS (mm/min)	IPT (°C)
Base 1	5.00	2	7.5	836	47
Base 2	5.00	2	7.5	836	47
Base 3	5.00	2	7.5	836	47
1	4.50	2	7.0	800	43
2	4.44	2	6.9	800	45
3	4.39	2	7.0	825	40
4	4.33	2	6.5	760	56
5	4.27	2	6.7	800	46
6	4.21	2	6.7	800	44
7	4.16	2	6.4	760	51
8	4.10	2	6.7	800	40
9	4.49	2	7.0	800	43
10	4.43	2	7.0	823	41
11	4.37	2	7.0	834	40
12	4.30	2	6.5	763	55
13	4.24	2	6.7	800	45
14	4.70	2	7.0	786	52
15	4.63	2	7.0	800	50
16	4.55	2	7.1	820	44
17	4.48	2	6.7	764	54
18	4.41	2	7.0	825	41
19	4.34	2	6.5	760	57
20	4.88	2	7.5	843	45
21	4.80	2	7.5	854	40
22	4.71	2	7.0	780	52
23	4.63	2	7.0	796	50
24	4.55	2	7.1	820	44
25	4.47	2	6.7	765	54
26	4.39	2	7.0	825	40
27	4.31	2	6.6	772	48
28	4.93	2	7.5	840	46
29	4.83	2	7.5	850	43
30	4.74	2	7.4	850	40
31	4.64	2	7.0	796	51
32	4.55	2	7.1	820	44
33	4.45	2	7.0	816	42
34	5.23	2	7.5	800	60
35	5.11	2	7.3	776	59
36	5.00	2	7.5	836	47

inside bead were deposited first to avoid collapse at the edge and then the rest of the weld beads were deposited successively. It is worth mentioning that the start point of each weld path is randomly designated so that the irregular bead shape can be spread out. After each weld path

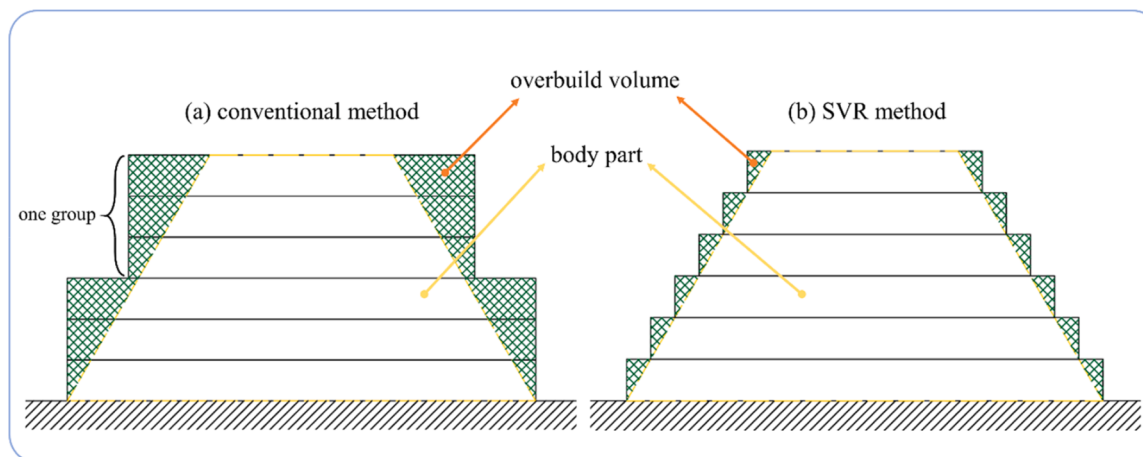


Fig. 13. The use of SVR bead modelling method can significantly reduce the scrap to be removed.

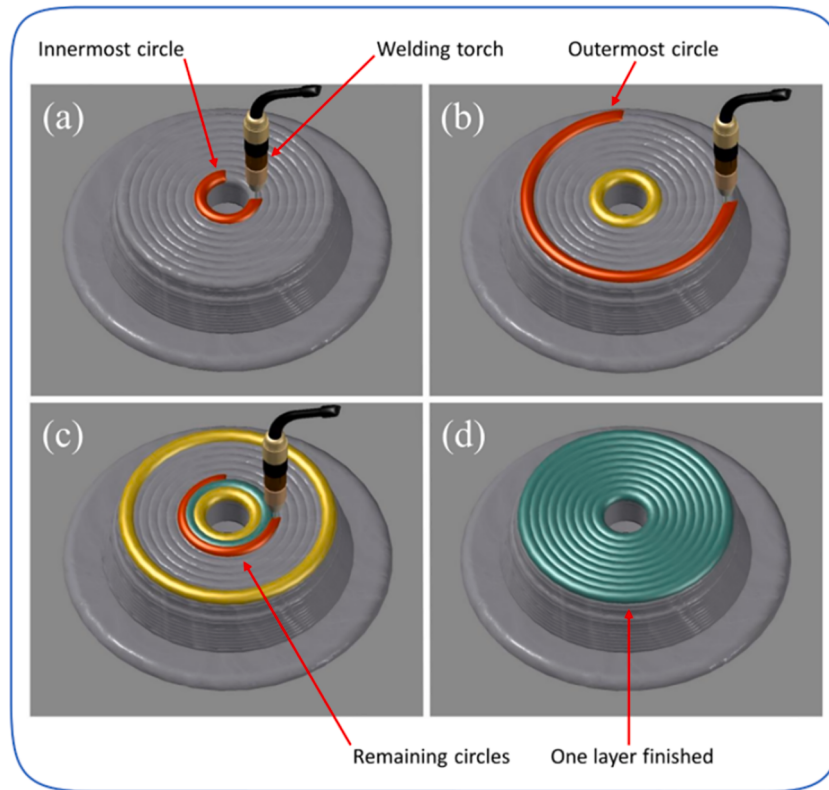


Fig. 14. The welding sequence of one layer. (a) the innermost circle is welded first, (b) the outermost circle is welded second, (c) then weld the remaining circles from inside to outside, (d) finish welding for one layer.

deposition, the pyrometer was controlled to measure the temperatures of the five randomly distributed points on the deposited path surface. Until the average temperature was cooled down to the certain range (IPT), the subsequent path deposition starts. During this case study, the IPT was set to be 40 to 60° centigrade to demonstrate the system is able to output welding parameters with user the preferred IPT.

After the deposition of each layer, the software took a photo of each layer to evaluate the performance of the proposed model. Fig. 15 shown the surface appearance of a few layers which were selected randomly. A smooth surface appearance indicates that layers are manufactured accurately with the predicted welding parameters. The surface of each layer was scanned for further assessment of the system, as an example shown in Fig. 16(a). The flat surface demonstrates there is no void and unacceptable humps for each layer. In addition, the surface waviness is quite stable for each layer which indicates the predicted OD are accurate. Moreover, heights around 2 mm with minor fluctuations were achieved for all layers as designated. Finally, the near-net shape of the final product is provided in Fig. 16(b), the overall geometry of the part is smooth without stair pattern on the surface. The performance of the proposed algorithm was validated through the case study.

5.2. Discussion

The performance of the proposed system can be summarized as follows,

- 1) **High model accuracy.** The proposed modelling method provides a high deposition accuracy for WAAM. Fig. 17 shows the error rate between predicted weld bead geometries and sampled weld bead geometries in the test. The MSE of OD and BH is 0.0474 and 0.0068 respectively, which demonstrates a high model accuracy. In addition, the accurate weld bead geometry control enables a smooth surface of each layer, as shown in Fig. 15. Finally, the final near-net

shape product is provided in Fig. 16, the successful fabrication of the workpiece demonstrates the performance of the proposed algorithm.

- 2) **Reduction in material waste and machining cost.** As illustrated in Fig. 13, the SVR algorithm can effectively reduce the material waste. In terms of the case study, the material waste is 7306 mm³ using the proposed SVR method compared to 40,646 mm³ using conventional bead modelling method (with 6 layers in one group). The material waste is reduced by 82.03% which saves 5.9% material total usage. In addition, the near-net shape of the final product indicates that the post-machining cost can be significantly reduced.
- 3) **High efficiency.** Compared to conventional weld bead methods, the proposed SVR based system can improve production efficiency due to (i) the entire process is executed automatically. Once the operator inputs the system setup, the system can automatically build the model from bead on plate deposition, data processing to bead model creation. The software can be provided to operators without much knowledge on WAAM or the welding process. (ii) The computation time of the welding parameters prediction is relatively short, only a few seconds using the machine learning algorithm. The short computation time is critical for depositing parts with complex geometries, where the welding parameters are required to be adjusted frequently.

6. Conclusion

This paper developed an automated weld bead modelling system for the WAAM using machine learning. The system is a novel backward model, which generates the optimal deposition parameters according to the desired weld bead geometry under various temperatures (IPT). An innovative predictive model had been established by using the SVR method for predicting welding parameters with minimum human operation. By using the proposed SVM based algorithm, weld bead models can be created with a high level of accuracy. Three critical

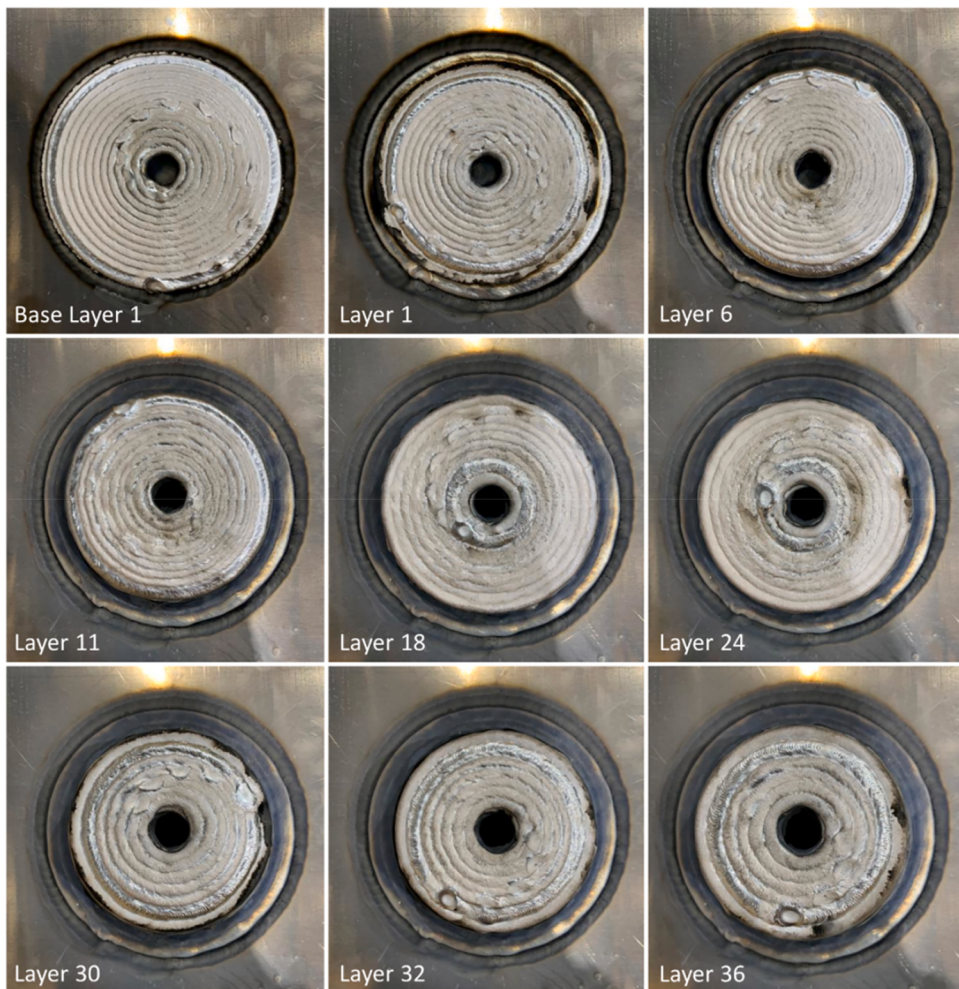


Fig. 15. Layer surface appearances of randomly selected layers.

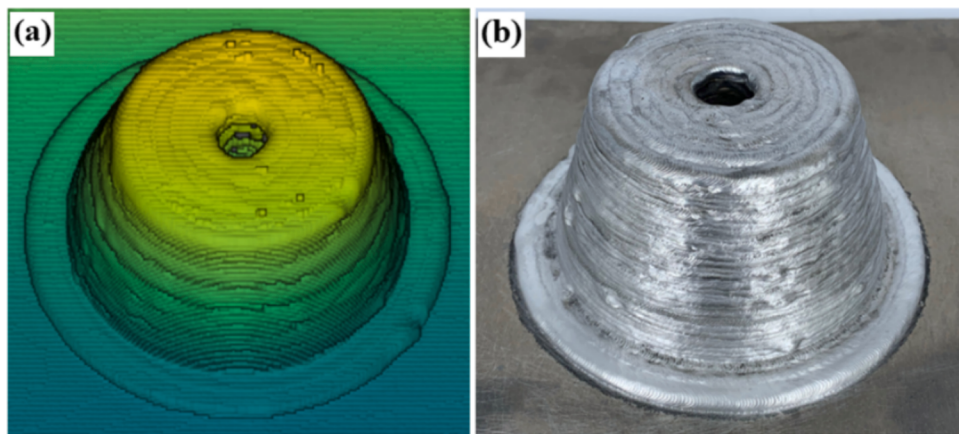


Fig. 16. (a) The 3D reconstruction image, (b) the final product.

modules of the system are summarized below,

- 1) *Data generation module.* The necessary training data are created through bead on plate deposition with sets of welding parameters. The system is able to deposit the welds, collect the weld bead geometry, and process the raw data for model creation.
- 2) *Model creation model.* The proposed SVRs algorithm is the most innovative part of this work. The algorithm can build up the

relationship between welding parameters and bead geometries accurately.

- 3) *Welding parameter generation module.* This module provides the optimal welding process parameters for the deposition process. The optimal welding parameters can be simply obtained through inputting the user preferred weld bead geometry.

Finally, the performance of the algorithm was validated by

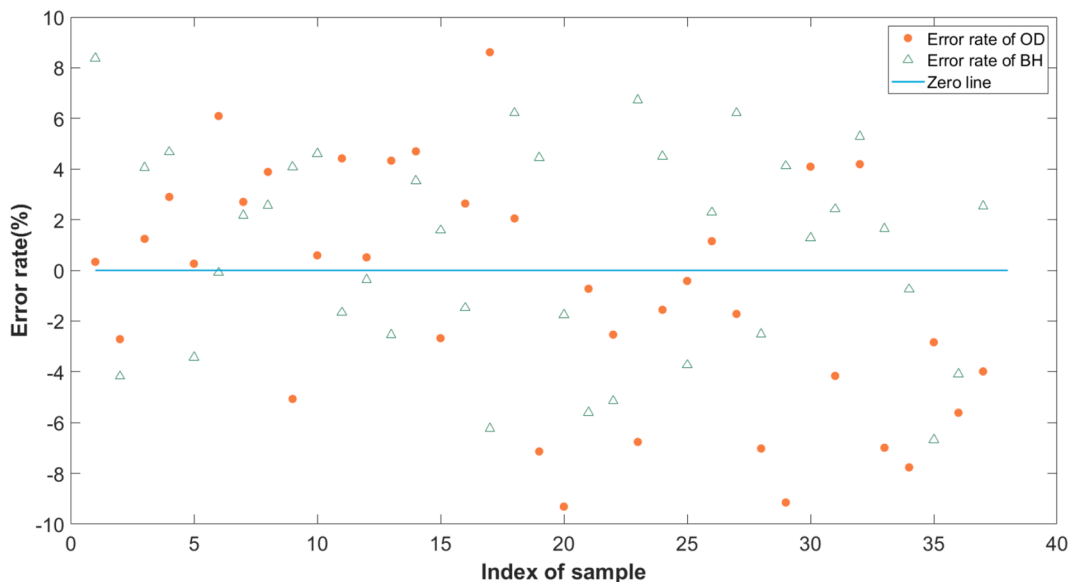


Fig. 17. The error rate between predicted data and sampled data in the case study test.

fabricating a metal part. The high quality of the workpiece shows the proposed model can provide optimal welding parameters for weld bead with different geometries in WAAM. In addition, the accurate model can help reduce the raw material usage which is critical for expensive metallic materials, such as titanium alloys typically used in aerospace industry.

CRediT authorship contribution statement

Donghong Ding: Formal analysis, Validation, Investigation, Resources. **Fengyang He:** Software, Writing - original draft, Data curation. **Lei Yuan:** Conceptualization, Writing - review & editing, Supervision. **Zengxi Pan:** Supervision, Project administration, Writing - review & editing. **Lei Wang:** Methodology, Writing - review & editing. **Montserrat Ros:** Writing - review & editing, Supervision.

Declaration of Competing Interest

The authors declare that they have no known competing financial interests or personal relationships that could have appeared to influence the work reported in this paper.

Acknowledgement

This work was supported in part by the National Natural Science Foundation of China under Grant 51805085 and in part by China Scholarship Council under Grant 201708200016, 202008200004.

Reference

- [1] Y. Cao, S. Zhu, X. Liang, W. Wang, Overlapping Model of Beads and Curve Fitting of Bead Section For Rapid Manufacturing By Robotic MAG Welding Process, 27, Robotics and Computer-Integrated Manufacturing, 2011, pp. 641–645.
- [2] H. Segerman, 3D printing for mathematical visualisation. The Mathematical Intelligencer, 2012, pp. 1–7.
- [3] P. Almeida, S. Williams, Innovative process model of Ti-6Al-4 V additive layer manufacturing using cold metal transfer (CMT), in: Proceedings of the Twenty-First Annual International Solid Freeform Fabrication Symposium, Austin, TX, USA, University of Texas at Austin, 2010.
- [4] D. Clark, M. Bache, M.T. Whittaker, Shaped metal deposition of a nickel alloy for aero engine applications, J. Mater. Process. Technol. 203 (2008) 439–448.
- [5] D. Ding, Z. Pan, D. Cuiuri, H. Li, A multi-bead overlapping model for robotic wire and arc additive manufacturing (WAAM), Robot. Comput. Integrat. Manuf. 31 (2015) 101–110.
- [6] Y. Li, Y. Sun, Q. Han, G. Zhang, I. Horváth, Enhanced beads overlapping model for wire and arc additive manufacturing of multi-layer multi-bead metallic parts, J. Mater. Process. Technol. 252 (2018) 838–848.
- [7] D. Ding, C. Shen, Z. Pan, D. Cuiuri, H. Li, N. Larkin, S. van Duin, Towards an automated robotic arc-welding-based additive manufacturing system from CAD to finished part, Comput. Aided Design 73 (2016) 66–75.
- [8] J. Xiong, G. Zhang, J. Hu, Y. Li, Forecasting process parameters for GMAW-based rapid manufacturing using closed-loop iteration based on neural network, Int. J. Adv. Manuf. Technol. 69 (2013) 743–751.
- [9] J.L. Prado-Cerdeira, J.L. Diéguez, A.M. Camacho, Preliminary development of a wire and arc additive manufacturing system (WAAM), Proc. Manuf. 13 (2017) 895–902.
- [10] P. Thamarasi, S. Ragunathan, E. Mohankumar, Robotics GMAW-weld bead geometry modeling using MATLAB script approach, Res. J. Appl. Sci., Eng. Technol. 9 (2015) 679–684.
- [11] F. Kolahan, M. Heidari, A new approach for predicting and optimizing weld bead geometry in GMAW, Int. J. Mech. Syst. Sci. Eng. 2 (2010) 138–142.
- [12] H. Geng, J. Xiong, D. Huang, X. Lin, J. Li, A prediction model of layer geometrical size in wire and arc additive manufacture using response surface methodology, Int. J. Adv. Manuf. Technol. 93 (2017) 175–186.
- [13] Y.-A. Song, S. Park, S.-W. Chae, 3D welding and milling: part II—optimization of the 3D welding process using an experimental design approach, Int. J. Mach. Tools Manuf. 45 (2005) 1063–1069.
- [14] D. Ding, Z. Pan, D. Cuiuri, H. Li, S. van Duin, N. Larkin, Bead modelling and implementation of adaptive MAT path in wire and arc additive manufacturing, Robot. Comput. Integrat. Manuf. 39 (2016) 32–42.
- [15] J. Xiong, G. Zhang, J. Hu, L. Wu, Bead geometry prediction for robotic GMAW-based rapid manufacturing through a neural network and a second-order regression analysis, J. Intell. Manuf. 25 (2014) 157–163.
- [16] A. Al-Faruk, A. Hasib, N. Ahmed, U.Kumar Das, Prediction of weld bead geometry and penetration in electric arc welding using artificial neural networks, Int. J. Mech. Mechatron. Eng. 10 (2010) 19–24.
- [17] C. Cortes, V. Vapnik, Support-vector networks, Mach. Learn. 20 (1995) 273–297.
- [18] R.M. Balabin, E.I. Lomakina, Support vector machine regression (SVR/LS-SVM)—An alternative to neural networks (ANN) for analytical chemistry? Comparison of nonlinear methods on near infrared (NIR) spectroscopy data, Analyst 136 (2011) 1703–1712.
- [19] B. Samanta, K. Al-Balushi, S. Al-Araimi, Artificial neural networks and support vector machines with genetic algorithm for bearing fault detection, Eng. Appl. Artif. Intell. 16 (2003) 657–665.
- [20] V. Cherkassky, Y. Ma, Practical selection of SVM parameters and noise estimation for SVM regression, Neural Netw. 17 (2004) 113–126.
- [21] H. Wang, D. Pi, Y. Sun, Online SVM regression algorithm-based adaptive inverse control, Neurocomputing 70 (2007) 952–959.
- [22] F. Kaytez, M.C. Taplamacioglu, E. Cam, F. Hardalac, Forecasting electricity consumption: a comparison of regression analysis, neural networks and least squares support vector machines, Int. J. Electr. Power Energy Syst. 67 (2015) 431–438.
- [23] B. Chen, H. Zhang, J. Feng, S. Chen, A study of welding process modeling based on Support Vector Machines, in: Proceedings of 2011 International Conference on Computer Science and Network Technology, IEEE, 2011, pp. 1859–1862.
- [24] L.D. Xu, Enterprise Integration and Information architecture: a Systems Perspective On Industrial Information Integration, CRC Press, 2014.
- [25] Y. Chen, Industrial information integration—a literature review 2006–2015, J. Indus. Inform. Integr. 2 (2016) 30–64.

- [26] Y. Chen, A survey on industrial information integration 2016–2019, *J. Indus. Integr. Manage.* 5 (2020) 33–163.
- [27] K. Derekar, J. Lawrence, G. Melton, A. Addison, X. Zhang, L. Xu, Influence of interpass temperature on wire arc additive manufacturing (WAAM) of aluminium alloy components, in: MATEC Web of Conferences, EDP Sciences, 2019, p. 05001.
- [28] H. Geng, J. Li, J. Xiong, X. Lin, Optimisation of interpass temperature and heat input for wire and arc additive manufacturing 5A06 aluminium alloy, *Sci. Technol. Weld. Join.* 22 (2017) 472–483.
- [29] B. Wu, Z. Pan, D. Ding, D. Cuiuri, H. Li, Z. Fei, The effects of forced interpass cooling on the material properties of wire arc additively manufactured Ti6Al4V alloy, *J. Mater. Process. Technol.* 258 (2018) 97–105.
- [30] J. Xiong, G. Zhang, H. Gao, L. Wu, Modeling of bead section profile and overlapping beads with experimental validation for robotic GMAW-based rapid manufacturing, *Robot. Comput. Integrat. Manuf.* 29 (2013) 417–423.
- [31] A.J. Smola, B. Schölkopf, A tutorial on support vector regression, *Stat. Comput.* 14 (2004) 199–222.
- [32] V. Cherkassky, Y. Ma, Comparison of model selection for regression, *Neural Comput.* 15 (2003) 1691–1714.
- [33] B.E. Boser, I.M. Guyon, V.N. Vapnik, A training algorithm for optimal margin classifiers, in: Proceedings of the Fifth Annual Workshop on Computational Learning Theory, ACM, 1992, pp. 144–152.
- [34] K.-j. Kim, Financial time series forecasting using support vector machines, *Neurocomputing* 55 (2003) 307–319.
- [35] F.E. Tay, L. Cao, Application of support vector machines in financial time series forecasting, *Omega (Westport)* 29 (2001) 309–317.
- [36] C.-C. Chang, C.-J. Lin, LIBSVM: a library for support vector machines, *ACM Trans. Intell. Syst. Technol. (TIST)* 2 (2011) 27.
- [37] S. An, W. Liu, S. Venkatesh, Fast cross-validation algorithms for least squares support vector machine and kernel ridge regression, *Pattern Recognit.* 40 (2007) 2154–2162.
- [38] K.M. Kanti, P.S. Rao, Prediction of bead geometry in pulsed GMA welding using back propagation neural network, *J. Mater. Process. Technol.* 200 (2008) 300–305.
- [39] Y. Zhang, X. Gao, S. Katayama, Weld appearance prediction with BP neural network improved by genetic algorithm during disk laser welding, *J. Manuf. Syst.* 34 (2015) 53–59.
- [40] N. Molayi, M.J. Eidi, Application of multiple kernel support vector regression for weld bead geometry prediction in robotic GMAW process, *Int. J. Electrical Comput. Eng.* 8 (2018) 2310.
- [41] I. Guyon, A. Elisseeff, An introduction to variable and feature selection, *J. Machine Learn. Res.* 3 (2003) 1157–1182.